CHAPTER-X

Physicochemical Study of Solution Behavior of Ionic Liquid Prevalent in Diverse Solvent Systems at Different Temperatures

X.1. INTRODUCTION

In existing times Ionic liquids (IL) have appeared as room temperature ionic liquids (RTILs) and atmosphere responsive solvents for the development of the manufacturing assemble of chemicals. Ionic liquids have been progressively more used for various commercial and potential applications such as organic synthesis, catalysis, electrochemical devices and solvent extraction of a variety of compounds. Most of the cases of ILs the cations may be organic or inorganic while the anions are inorganic [1]. Now a days the large attention in ionic liquids was commenced because of its usefulness as eco-friendly "green" solvents [2,3]. Ionic liquids offer the advantage of both homogeneous and heterogeneous catalysts. This is because preferred ionic liquids can be immiscible with the reactants and products but dissolve the catalysts. Enzymes are also stable in ionic liquids, opening the possibility for ionic liquids to be used in biological reactions, such as the synthesis of pharmaceuticals [4,5]. Ionizing radiation does not affect ionic liquids, so they could even be used to treat high-level nuclear waste. Ionic liquids can selectively dissolve and remove gases and could be used for air purification on submarines and spaceships. Ionic liquid used in the present widely used in solvent extraction, liquid–liquid extraction process, electrochemical studies, dye-sensitized solar cells [6-9]. Moreover, good thermal stability, variable viscosity, no effective vapor pressure, recyclability and conventional organic solvents have been replaced by ILs in organic synthesis is also great qualities of IL [10-12].

Published in Chem. Phys. Lett. (2016) 665 85-94

The utilized solvents in this study ascertain broad industrial usage. Acetonitrile (ACN) is largely used in battery industries and also used in pharmaceutical, perfume, rubber product, pesticide, acrylic nail remover preparation industries. For animal fatty acids and vegetable oils extraction ACN is chiefly used. Tetrahydrofuran (THF) is mainly used as a precursor to polymers. The other major applications of THF are an industrial solvent for PVC and in vernishes. 1,3-Dioxolane (DO) is a lower toxic versatile aprotic solvent. The oxygen atom present in DO acts as Lewis base, so it is able to solvate many inorganic compounds. DO is a very good industrial solvent which used prominently in the high energy battery industries and finds application in organic synthesis as manifested from the physicochemical studies in this medium [13]. Different standard compositions of the ionic liquid and the solvents taken can be used in the battery industry, dye industry and in many more industries. Thus, this work has a valuable contribution to these industries. These new solvent mixtures can make the products cheaper, easily available and more useful.

Currently physical chemists have long been of intense attention to the electrochemical study. The study of transport property is a helpful tool for understanding the performance of ions in solution. Furthermore, acquaintance of the thermodynamic properties is indispensable for the proper plan of industrial progressions. In both the theoretical and applied research areas have huge consequence of the perfect knowledge of thermodynamic properties of solution mixtures. In electrolyte solution systems the molecular interaction is afforded through the measurements of the bulk properties, such as density and viscosity of liquids. The above studies help us to understand the behaviour of IL in diverse solvent systems. Ion–ion and ion–solvent communications can be developed as a way to study on the apparent and partial molal volumes of the electrolyte and the dependence of viscosity on the concentration of electrolyte [14].

In continuation our earlier studies [15,16] an attempt has been made in this present study we have done the conductivity, density, viscosity and FTIR study of an IL, 1-butyl-4-methylpyridinium hexafluorophosphate ([bmpy]PF_6) in industrially imperative

solvents at three different temperatures to explore the solvation consequences of IL in diverse solvent systems.

X.2. EXPERIMENTAL

X.2.1 Source and purity of samples

In this current research work, the chosen IL puriss grade was purched from Sigma-Aldrich, Germany and was used as purchased. The mass fraction purity of the ILs was ≥ 0.99.

All the spectroscopic grade solvents having mass fraction of purity 0.995 were procured from Sigma-Aldrich, Germany and were used as procured. The IL was preserved in vacuum desiccator containing anhydrous P_2O_5 and any water content of the solvents was removed by using molecular sieves. The literature values as shown in Table X.1 were in excellent concurrence with assessment of measured density, viscosity and conductivity values of IL, which verified the purity [17] of the IL.

X.2.2 Apparatus and Procedure

All the stock solutions of the IL in considered solvents were prepared by mass (weighed by Mettler Toledo AG-285 with uncertainty 0.0003 g). In case of conductometric study the working solutions were achieved by mass dilution of the stock solutions.

Temperature of the solution was maintained to within ± 0.01 K using Brookfield Digital TC-500 temperature thermostat bath. The viscosities were measured with an accuracy of ± 1 %. Each measurement reported herein is an average of triplicate reading with a precision of 0.3 %.

The conductance measurements were carried out in a Systronics-308 conductivity bridge of accuracy ±0.01%, using a dip-type immersion conductivity cell, CD-10 having a cell constant of approximately (0.1 ± 0.001) cm^{-1}. Measurements were made in a thermostat water bath maintained at T = (298.15 ± 0.01) K. The cell was calibrated by the method proposed by Lind et al.[18] and cell constant was calculated based on 0.01

(M) aqueous KCl solution. During the conductance measurements, cell constant was maintained within the range 1.10–1.12 cm^{-1}. The conductance data were reported at a frequency of 1 kHz and the accuracy was ±0.3%. During all the measurements, uncertainty of temperatures was ±0.01 K.

The density values of the solvents and experimental solutions (ρ) were measured using vibrating u-tube Anton Paar digital density meter (DMA 4500M) with a precision of ±0.00005 g cm^{-3} maintained at ±0.01 K of the desired temperature. It was calibrated by triply-distilled water and passing dry air.

The viscosity values were measured by means of a Brookfield DV-III Ultra Programmable Rheometer with fitted spindle size-42 fitted to a Brookfield digital bath TC-500. The viscosities were obtained using the following equation

$$\eta = (100 / RPM) \times TK \times \text{torque} \times SMC$$

where *RPM*, *TK* (0.09373) and *SMC* (0.327) are the speed, viscometer torque constant and spindle multiplier constant, respectively. The instrument was calibrated against the standard viscosity samples supplied with the instrument, water and aqueous $CaCl_2$ solutions [19]. The viscosities were measured with an accuracy of ± 1 %.

Fourier-transform infrared (FT-IR) was carried out on a Perkin Elmer FT-IR spectrometer (Spectra RXI) with sample prepared as 0.05 (M) solution of IL in the studied solvent systems. The spectra were acquired in the frequency range 4000–400 cm^{-1} at a resolution of 4 cm^{-1} with a total of 16 scans.

X.3. RESULTS AND DISCUSSION

Table X.1 demonstrates the solvent properties. The concentrations and molar conductances (Λ) of IL in ACN, THF and DO at 298.15, 303.15 and 308.15 K temperature are presented in Table S1. Due to diverse temperature based systems the molal conductance (Λ) has been acquired from the specific conductance (κ) value using the following equation.

$$\Lambda = (1000\ \kappa) / m \qquad (1)$$

Linear conductance curve (Λ vs $\sqrt{m}$) was achieved for the electrolyte in ACN extrapolation of $\sqrt{m} = 0$ evaluated the starting limiting molar conductance for the electrolyte. In conductometric study of IL in THF and DO triple-ion formation occurs. As there is the formation of the cluster in the concentrated solutions, we have discussed the conductometric study in the dilute solutions of the IL and the different solvents taken [20].

X.3.1. Ion-pair Formation

In conductometric study of ([bmpy]PF_6) in ACN the ion-pair formation is investigated using the Fuoss conductance equation [21]. Three adjustable parameters, i.e., Λ_0, K_A and R have been derived from the Fuoss equation using a given set of conductivity values (c_j, Λ_j; j = 1…….n). At this point, Λ_0 is the limiting molar conductance, K_A is the observed association constant and R is the association distance, i.e., the maximum centre to centre distance between the ions in the solvent separated ion-pairs. There is no particular method [22] to determine the R value but in order to treat the data in our system, R value is alleged to be, $R = d + a$, where d refers the average distance consequent to the side of a cell engaged by a solvent molecule and a refers the summation of the crystallographic radii of the ions. The distance, d refers above is specified as,

$$d = 1.183 \left(M / \rho\right)^{1/3} \quad (2)$$

where, M and ρ refer the molecular mass and the density of the solvent respectively.

Therefore, the Fuoss conductance equation may be embodied as follows:

$$\Lambda = P\Lambda_o[(1+R_X)+E_L] \quad (3)$$

$$P = 1-\alpha(1-\gamma) \quad (4)$$

$$\gamma = 1-K_A m\gamma^2 f^2 \quad (5)$$

$$-\ln f = \beta\kappa / 2(1+\kappa R) \quad (6)$$

$$\beta = e^2 / \left(\varepsilon_r k_B T\right) \quad (7)$$

$$K_A = K_R / (1-\alpha) = K_R / (1+K_S) \quad (8)$$

where, Λ_0 is the limiting molal conductance, K_A is the observed association constant, R is the association distance, R_X is the relaxation field effect, E_L is the electrophoretic counter current, k is the radius of the ion atmosphere, ε is the relative permittivity of the solvent mixture, e is the electron charge, m is the molality of the solution, k_B is the Boltzmann constant, K_S is the association constant of the contact-pairs, K_R is the association constant of the solvent-separated pairs, γ is the fraction of solute present as unpaired ion, α is the fraction of contact pairs, f is the activity coefficient, T is the absolute temperature and β is twice the Bjerrum distance.

The computations were executed using the program recommended by Fuoss. The initial Λ_0 values for the interaction process were obtained from Shedlovsky extrapolation of the data [23]. Attempt for the program is the no. of data, n, followed by ε, η (viscosity of the solvent), initial Λ_0 value, T, ρ (density of the solvent), mole fraction of the first component, molar masses, M_1 and M_2 along with m_j, Λ_j values where j = 1, 2…….n and an instruction to cover preselected range of R values.

Actually, estimates are executed through ruling the values of Λ_0 and α which minimize the standard deviation, δ, whereby

$$\delta^2 = \sum [\Lambda_j(cal) - \Lambda_j(obs)]^2 / (n - m) \qquad (9)$$

for a sequence of R values and then plotting δ against R, the best- fit R corresponds to the minimum of the δ–R versus R curve. So, an approximate sum is made over a fairly wide range of R values using 0.1 increment to locate the minimum but no significant minima is found in the δ - R curves, thus R values is assumed to be $R = d + a$, with terms having usual significance. Finally, the corresponding limiting molar conductance (Λ_o), association constant (K_A), co-sphere diameter (R) and standard deviations of experimental Λ (δ) achieved from Fuoss conductance equation for ([bmpy]PF_6) in ACN at 298.15, 303.15 and 308.15K are given in Table X.2. The variation of equivalent conductance with square root of concentrations for ACN has been shown in Figure X.1 (Scheme X.2).

The standard Gibbs free energy change of solvation, ΔG^o, for ([bmpy]PF_6) in ACN can be determined with help of the following equation [24],

$$\Delta G^{o} = -RTlnK_{A} \quad (10)$$

The perusal of Table X.3 shows that the value of Gibbs free energy is entirely negative in ACN at all the three studied temperatures. It can also be enlightened by considering the participation of specific non-covalent interaction such as electrostatic forces of attraction, van der Walls forces etc. in the ion-association process (Scheme X.3).

The increase in the values of ΔG^{o} of IL in ACN with increasing temperatures show that degree of association is lower with the increase of temperatures. Commencing the scrutiny of Table X.2 it may be concluded that Λ_o increases with increase in temperature while K_A value decreases with increase in temperature for IL in ACN. It be originate that ΔG^{o} decreases the negativity with increasing the temperature which indicates the spontaneity of the ion-association process.

By use of tetrabutylammonium tetraphenylborate (Bu_4NBPh_4) as a "reference electrolyte" [25] the ionic conductancs $\lambda_0^{\pm}$ (for $[bmpy]^+$ cation and $[PF_6]^-$ anion) were derived in solvent ACN. The values of ionic conductance $\lambda_0^{\pm}$ and the product of ionic conductance and viscosity of the solvent named ionic Walden product $(\lambda_0^{\pm}\eta)$ along with Stokes' radii (r_s) and Crystallographic Radii (r_c) of $[bmpy]PF_6$ in ACN at different temperatures are given in Table X.4.

Ion-solvation can also be explained with the help of another characteristic property called the Walden product [26] ($\Lambda_0.\eta$) (Table X.3). Λ_0 increases for the electrolyte in ACN with increasing temperature and the $\Lambda_0.\eta$ also increases even though the viscosity of the solvent decreases. This fact indicates the prevalence of Λ_0 over η.

X.3.2. Thermodynamic parameters

The variation of conductance of an ion with temperature can be treated as similar to the variation of the rate constant with temperature which is given by the Arrhenius equation [27],

$$\Lambda_o = A.e^{-E_a/RT} \quad (11)$$

$$\log \Lambda_o = \log A - \frac{E_a}{2.303RT} \quad (12)$$

Where A is an Arrhenius constant, E_a is the activation energy of the rate process which determines the rate of movement of ions in solution. The slope of the linear plot of $\log \Lambda_o$ Vs 1/T (Fig not shown) gives the value of E_a (Table X.5). From the Arrhenius equation it has been found that activation energy is positive. This indicates the higher mobilities of ions in solution increases. So Λ_o (limiting conductance) value increases with increase in temperature. Conductance of an ion is dependent on the rate of movement of ion. Here the changes of number of ions are not accounted quantitatively but, due to the formation of ion-pair available number of free ion will decrease and consequently molar conductivity of the solution decreases.

Thermodynamic parameters of association such as ΔH_a, ΔG_a and ΔS_a were also calculated on the basis of the following equations

$$\Delta H_a = \frac{RT^2 \ln K_a}{dT} \quad (13)$$

$$\Delta G_a = -RT \ln K_a \quad (14)$$

$$\Delta S_a = \frac{\Delta H_a - \Delta G_a}{T} \quad (15)$$

The change in enthalpy of the process of association (ΔH_a) is calculated from the slope of the plot of log Ka Vs 1/T (Fig not shown). ΔG_a was calculated at various temperatures and the average value was considered. ΔS_a was obtained from equation (15) at different temperatures and the average value was noted down. From the perusal of Table X.5 it can be assumed that the negative value of ΔG_a indicates the spontaneity of the ion-association process. The positive value of ΔH_a indicates that the ion-association processes are endothermic. The positive value of ΔS_a indicates the randomness increases from lower temperature to higher temperature.

X.3.3. Triple-ion Formation

There are several numbers of models which show the minimum value of equivalent conductivity of an electrolyte solution as the function of concentration by concerted fundamental studies including the pioneering work of Kohlrausch, Walden, Debye-Huckel and Fuoss-Kraus [28]. Since dielectric constant is dependent on several factors [29], there is clarity in ion-transport property governed by salt concentration.

According to Kohlrausch an empirical description was developed focusing on the concentration dependence of the molar conductivity. By the theoretical basis of this theory further developed by Debye- Hückel –Onsager considered that an ionic cloud is present about the central ion. Afterward including the effects of electrophoresis, the relaxation field and finite ion sizes Fuoss have been changed this model.

There may present a range of cation-anion interactions that result in what is somewhat slackly named as “ionic association”. These interactions effect in extensive survival and discrete ionic species whose existence can be spectroscopically identified. The power of these interactions leads to electronic redistribution within bonds that result in the shifts of normal mode frequency.

Fuoss and Kraus at first described the typical behavior of ionic conductance of ionic species in solvents having low dielectric constant. In case of low dielectric constant ($\varepsilon<10$) solutions at very dilute region with increasing salt concentration decrease of Λ attributed as ion-pair formation or solvent separated ion-pairs. The decrease of Λ at high salt conc. is usually attributed to the increase of bulk viscosity in the liquids [30]. This increase has been attributed to the formation of charged triple-ion aggregates (Figure X.2) [31].

Now the conductivity values of ACN, THF and dioxane are tried to fit in Fouss ion-pair formation equation but, only the ACN conductivity values are fitted properly. Hence, the conductivity values of THF and dioxane are tried to fit in Fouss triple-ion formation equation and gives the concerned proper values obtained from Fouss triple-ion formation equation. So, we can say that in our studied systems (THF and dioxane) among many models triple-ion formation occurs. So, it can be explicitly state that here

we employed the triple ion model with no reasons other than that the fitting worked well.

For this IL in THF and DO solvent system the conductance data have been analysed using the classical Fuoss-Kraus equation [31] for triple-ion formation,

$$\Lambda g(c)\sqrt{c} = \frac{\Lambda_0}{\sqrt{K_p}} + \frac{\Lambda_0^T K_T}{\sqrt{K_p}}\left(1 - \frac{\Lambda}{\Lambda_0}\right)c \tag{16}$$

$$g(c) = \frac{\exp\{-2.303\ \beta'(c\Lambda)^{0.5}/\Lambda_0^{0.5}\}}{\{1 - S(c\Lambda)^{0.5}/\Lambda_0^{1.5}\}(1 - \Lambda/\Lambda_0)^{0.5}} \tag{17}$$

$$\beta' = 1.8247\times10^6/(\varepsilon T)^{1.5} \tag{18}$$

$$S = \alpha\,\Lambda_0 + \beta = \frac{0.8204\times10^6}{(\varepsilon T)^{1.5}}\Lambda_0 + \frac{82.501}{\eta(\varepsilon T)^{0.5}} \tag{19}$$

In the above equations, Λ_0 is the sum of the molar conductance of the simple ions at infinite dilution; Λ_0^T is the sum of the conductances of the two triple ions $bmpy^+PF_6^-$ and $bmpy^+(PF_6)_2^-$. $K_P \approx K_A$ and K_T are the ion-pair and triple-ion formation constants. To make equation (16) applicable, the symmetrical approximation of the two possible constants of triple ions equal to each other has been adopted [32] and Λ_0 values for the studied electrolytes have been calculated. Λ_0^T is calculated by setting the triple ion conductance equal to $2/3\Lambda_0$ [33].

During linear regression analysis of equation (16) the ratio Λ_0^T/Λ_0 was set equal to 0.667. Table 6 demonstrates the limiting molar conductance of triple-ions (Λ_0^T), slope and intercept of Eq. (16) for [bmpy]PF_6 in THF and DO at different temperatures. By the inspection of Table X.6 and Figure X.2 it may be stated that the limiting molar conductance (Λ^0) of [bmpy]PF_6 is higher in THF than in DO.

Linear regression analysis of equation (16) for the electrolyte in THF and DO with an average regression constant, R^2 = 0.9653, gives intercepts and slopes. These permit the calculation of other derived parameters such as K_P and K_T listed in Table X.7. It is observed that Λ passes through a minimum as c increases. The K_P and K_T values predict that major portion of the electrolyte exists as ion-pairs with a minor portion as triple-

ions (neglecting quadrupoles). Since the value of log (K_T/K_P) is found to be higher in DO than in THF, DO has privileged affinity of triple ion formation than THF.

Electrostatic ionic interactions become very large when permittivity of the solvent is very low (less than 10). In this situation ion-pairs present in solution attract the free +ve and -ve ions of the same medium. Due to the minimum distance of closest approach of the ions in lower permittivity media there is a possibility of greater aggregation by H-bonding [34,35]. The extent of triple-ion formation increases with decreasing the permittivity of the solvent. The above described phenomena exhibit triple-ion formation, which achieve the charge of the relevant ions in the concerned solution system [36] i.e.,

$$M^+ + Y^- \leftrightarrow M^+ \cdots\cdots Y^- \leftrightarrow MY \quad (20)$$

$$MY + M^+ \leftrightarrow MYM^+ \quad (21)$$

$$MY + Y^- \leftrightarrow MYY^- \quad (M= bmpy \text{ and } Y= PF_6) \quad (22)$$

Due to the formation of ternary association in THF and DO triple-ion removes some non-conducting species from solution system. So, after the achievement of minimum conductance values up to a certain concentrations then increase which is manifested by the non-linear conductance curves for the electrolyte in THF and DO.

Moreover, the ion-pair and triple-ion concentrations, c_P and c_T respectively of the electrolyte have also been calculated at the minimum conductance concentration of [bmpy][PF_6] in THF and DO using the following relations: [37]

$$\alpha = 1 / (K_P^{1/2} \cdot c^{1/2}) \quad (23)$$

$$\alpha_T = (K_T / K_P^{1/2}) \, c^{1/2} \quad (24)$$

$$c_P = c(1- \alpha - 3\alpha_T) \quad (25)$$

$$c_T = (K_T / K_P^{1/2}) \, c^{3/2} \quad (26)$$

Here α and α_T are the fractions of ion-pairs and triple-ions present in the salt-solutions respectively and are given in Table X.8. From Table X.8, it is observed that with increasing temperature the number of free ions per unit volume decreases resulting in an increase of K_P and K_T values. Thus, the values of C_P and C_T given in Table

X.8 indicate that the ions are mainly present as ion-pairs even at high concentration and a small fraction existing as triple-ions. With increasing the temperature C_P and C_T values increase and both C_P and C_T values are higher in THF than in DO.

The ion-solvent interaction of IL in DO is higher than in THF and ACN due to the interaction between The N atom of IL with two, one O atom of DO and one N atom of THF (Scheme X.1). From conductivity values it came to know that ion-solvent interaction occurs between the IL and the corresponding solvents. Ion-pair is formed in between IL and ACN and in THF and DO triple-ion is formed (Scheme X.2). Through the conductivity measurements we found the trend of association of IL with diverse solvent systems DO>THF>ACN.

X.3.4. Apparent molar volume

The density and viscosity values of [bmpy]PF_6 in ACN, THF and DO at 298.15, 303.15 and 308.15K respectively are stated in Table S2. At a particular temperature the density values of electrolyte in various solvent systems increase linearly with increasing the concentration of electrolyte. However the density values of IL in a particular solvent systems decreases with increase of temperature. By means of the following equations the apparent molar volumes ϕ_V were determined from the density values of solutions (Table S2).

$$\phi_V = M/\rho - (\rho - \rho_o)/m\rho_o\rho \qquad (22)$$

where M is the molar mass of the solute, m is the molality of the solution, ρ and ρ_0 are the densities of the solution and solvent, respectively. The apparent molar volumes ϕ_V were found to decrease with increasing molality (m) of IL in different solvents and increase with increasing temperature for the system under study. The limiting apparent molar volumes ϕ_V^0 were calculated using a least-squares treatment to the plots of ϕ_V versus $\sqrt{m}$ using the following Masson equation [38]

$$\phi_V = \phi_V^0 + S_V^* \cdot \sqrt{m} \qquad (23)$$

where ϕ_V^0 is the limiting apparent molar volume at infinite dilution and S_V^* is the experimental slope.

The plots of ϕ_V Vs square root of the molar concentration ($\sqrt{c}$) were found to be linear with negative slopes. The values of ϕ_V^0 and S_V^* are shown in Table X.9, reveals that ϕ_V^0 values for this electrolyte are generally positive [39] in all the solvent systems and is highest in DO. The variation of ϕ_V^0 values for this studied IL in different solvent systems at different temperatures has shown in Figure X.3. This indicates the presence of strong ion–solvent interactions of IL in DO. The extent ion-solvent interaction is highest in DO and in ACN ion-solvent interaction is lowest (scheme X.4).

In contrast, the S_V^* values designate the extent of ion-ion interaction. All the S_V^* values are negative, which indicates the presence of less ion-ion interaction in the medium. Such S_V^* values also show that extent of ion-ion interactions are highest in case of ACN and are lowest in DO. The above facts reveal that ion-solvent interactions govern over ion-ion interactions in all the studied solvent systems. According to Gurney co-sphere overlap model here overlap of the co-spheres of two ions form positive volume change. This result supports that higher values of ϕ_V^0 in DO sustain the higher ion-solvent interaction [40]. This fact lead to lower conductance of [bmpy]PF_6 in DO than in THF and ACN as conferred in above section. With increasing the temperature ϕ_V^0 values increase and S_V^* values decrease in every solution which indicates higher ion-solvent interaction than ion-ion interaction.

X.3.5. Temperature dependent limiting apparent molar volume:

The variation of ϕ_V^0 with the temperature of the IL in different solvents can be expressed by the general polynomial equation as follows,

$$\phi_V^0 = a_0 + a_1 T + a_2 T^2 \qquad (24)$$

where a_0, a_1, a_2 are the empirical coefficients depending on the solute, mass fraction (w_1) of IL, and T is the temperature range under study in Kelvin. The values of these coefficients of the above equation for the IL in ACN, THF and DO are reported in Table X.10.

The limiting apparent molar expansibilities, ϕ_E^0, can be obtained by the following equation,

$$\phi_E^0 = \left(\delta \phi_V^0 / \delta T\right)_P = a_1 + 2a_2 T \qquad (25)$$

The limiting apparent molar expansibilities, ϕ_E^0, change in magnitude with the change of temperature. The values of ϕ_E^0 of the studied IL at (298.15, 303.15, and 308.15) K are accounted in Table X.10. The table reveals that ϕ_E^0 is positive for IL in all the studied solvents and studied temperatures. This fact can ascribed to the absence of caging or packing effect for the IL in solutions.

Hepler [41] built-up a method to examine the sign of $\left(\delta \phi_E^0 / \delta T\right)_P$ for the solute in terms of the structure-making and -breaking capability of the solute in diverse solvent systems using the under mentioned general thermodynamic expression,

$$\left(\delta \phi_E^0 / \delta T\right)_P = \left(\delta^2 \phi_V^0 / \delta T^2\right)_P = 2a_2 \qquad (26)$$

The molecule is a structure maker when the sign of $\left(\delta \phi_E^0 / \delta T\right)_P$ is positive or a small negative; if not, then it is a structure breaker [42]. From Table X.11, it is manifested that $\left(\delta \phi_E^0 / \delta T\right)_P$ values for the considered IL in all the solvents are small negative. This fact predominately shows the structure making tendency of IL in concerned solution systems. Further here effects of electrostriction are accounted due to variation of temperature. With increasing temperature the electrostriction effect of ions increases and electrostricted solvent molecules would be released which consign the structure breaking capacity.

X.3.6. Viscosity calculation

The comparison and conformation of solvation of the electrolyte in the solvent systems can be explored very simply by viscosity measurement. Here we use the following Jones-Dole equation [43] to evaluate the viscosity data

$$\left(\eta/\eta_0 - 1\right)/\sqrt{c} = A + B\sqrt{m} \qquad (27)$$

where η and η_0 are the viscosities of the solution and solvent respectively. Table X.9 shows the values of viscosity *B*- and *A*- coefficients, obtained from the straight line by plotting $\left(\eta/\eta_0 - 1\right)/\sqrt{m}$ vs $\sqrt{m}$. Viscosity *B*-coefficient is an important device to offer information concerning the solvation of the solutes and their effects on the structure of the solvent. The viscosity B-coefficient reflects the quantitative ion–solvent interactions in the solution. A perusal of Table X.9 and Figure X.4 shows that the values of the *B*-coefficient are positive [44]. It suggests the presence of strong ion-solvent interactions which reinforce the increase of solvent viscosity value. The decrease of *A*-coefficient with increase of temperature shows very weak solute-solute interactions. The viscosity *A* and *B*-coefficients are in excellent agreement with the results drawn from the conductance and volumetric studies.

The values of the *B*- and *A*-coefficient obtained from viscometric measurement support the ϕ_V^0 and S_V^* values respectively obtained from the volumetric study. The viscosity B-coefficient is an expensive tool to provide information concerning the solvation of solutes and their effects on the structure of the solvent in the local vicinity of the solute molecules. Positive values of the B-coefficient (Table X.9) of IL in the studied solvent systems evident the presence of strong ion–solvent interactions and these types of interactions are strengthened from ACN to DO in the solvent mixtures. These conclusions are in excellent agreement with those drawn from ϕ_V^0 values discussed earlier. Due to the association of solvated solute molecules by the solvent molecules through solute-solvent interaction a resistance occur. So, viscosity *B*-coefficient values become higher in viscous solution system. With the elevation of temperature this type of interactions are strengthened [40]. From the accord of the

above discussions, it may be stated that, the solute-solvent interaction occurs by several types of interaction procedure such as hydrogen-bonding, dipole–dipole and solvophobic interactions [45]. At higher viscosity the triple-ion formation becomes more significant. In this situation, due to the formation of triple-ion equivalent conductivity starts increasing after passing through a minimum value.

The viscosity *B*- and *A*- coefficients are in superb concurrence with the results drawn from the volumetric studies. The ion-solvent interaction is highest in case of DO and lowest in ACN.

X.3.7. FTIR Spectroscopic Study

Molecular interface between IL and miscellaneous solvent systems can be qualitatively interpreted with the aid of FTIR spectroscopy. In case of ion-solvent and solvent-solvent interactions it is used as a supportive confirmation for the bond infringement and bond development (electrostatic bond) study. Table X.12 shows measured IR stretching frequencies of the functional groups of the pure solvents as well as the solutions of mixture ([bmpy]PF_6+Solvents).

For ACN the C≡N stretching vibration shows a sharp peak at ν_o = 2251.9 cm^{-1}. Mixture of ACN and IL (i.e. [bmpy]PF_6+CH_3CN) shows a peak at ν_s = 2275.1 cm^{-1}. Due to the distraction of dipole-dipole interface present in acetonitrile [46] and construction of ion-dipole interface between $[bmpy]^+$ and PF_6^- ions with C≡N bond the shift of C≡N stretching frequency is occurred. The change in stretching frequency of C-H bond [47] is 3.4 cm^{-1} of CH_3CN is negligible which shows that C-H bond does not contribute in interaction.

A sharp peak for C–O is obtained at 1042.8 cm^{-1} in case of THF. After addition of IL this peak shifts to 1061.6 cm^{-1}, due to the interaction of $[bupy]^+$ with the C–O dipole [47]. The ion–dipole interaction is formed due to the distraction of the H-bonding interface in the THF molecules. The change in stretching frequency of C-H bond 2.6 cm^{-1} of THF shows negligible contribution of C-H group.

After the addition of IL in DO the peak for C–O at 1158.2 cm^{-1} shift to 1175.5 cm^{-1}. Due to an ion–dipole interaction between $[bmpy]^+$and the C–O dipole the shift of C-O peak is arised. The change in stretching frequency of C-H bond 2.3 cm^{-1} of DO again shows negligible contribution of C-H group.

In view of the observed derived parameter the ion-solvation happening in studied solution systems {[bmpy][PF_6]+Solvent} have been represented in Scheme X.4.

IV.4. CONCLUSION

Commencing the prevalent study of the IL, [bmpy]PF_6 in different solvent systems it leads to conclude that the IL is more associated in DO than in THF and ACN. The results originated from the conductometric study evidently demonstrate that the IL in DO and THF mostly remains as triple-ions rather than ion-pairs, but in ACN the IL remains as ion-pairs. The investigational assessments achieved form the volumetric and viscometric studies at different temperatures also afford the similar concurrence as derived from the study of transport property. Further, due to the diverse permittivity of the inspected solvents the extent of ion-solvent interaction of [bmpy]PF_6 is amplified in the following order:

DO>THF>ACN

TABLES

Table X.1: Density (ρ), viscosity (η), relative permittivity (ε) and Conductance (Λ) of the different solvents Acetonitrile, Tetrahydrofuran and 1,3 Dioxolane at different temperatures[a].

Temp.	$\rho^a \cdot 10^{-3}$/kg m^{-3}	η^a/mPa s	ε	$\Lambda^a \cdot 10^4$/S m^2 mol^{-1}
		Acetonitrile		
298.15	0.78601	0.35	35.94	0.0695
303.15	0.78283	0.34	35.01	0.0702
308.15	0.78005	0.33	34.30	0.0705
		Tetrahydrofuran		
298.15	0.88611	0.48	7.58	0.0677
303.15	0.88596	0.44	7.24	0.0683
308.15	0.88583	0.40	7.09	0.0687
		1,3 Dioxolane		
298.15	1.05877	0.59	7.34	0.0659
303.15	1.05870	0.57	7.18	0.0664
308.15	1.05862	0.53	7.02	0.0669

[a] Standard uncertainties u are: $u(\rho)$=±5×10^{-5} g·cm^{-3}, $u(\eta)$=± 1 %, $u(\Lambda)$=±0.01% and $u(T)$ =±0.01K

Table X.2: Limiting molar conductance (Λ_o), association constant (K_A), co-sphere diameter (R) and standard deviations of experimental Λ (δ) obtained from Fuoss conductance equation of [bmpy]PF_6 in Acetonitrile at 298.15 K, 303.15 K and 308.15 K respectively.

T/K	$\Lambda_o \cdot 10^4$/S·m^2·mol^{-1}	K_A/ dm^3·mol^{-1}	R/Å	δ
298.15	188.77	713.48	9.54±0.10	3.58
303.15	196.61	633.28	9.42±0.10	3.48
308.15	203.36	565.45	9.33±0.10	4.02

Table X.3: Walden product ($\Lambda_o \cdot \eta$) and Gibb's energy change (ΔG°) of [bmpy]PF_6 in Acetonitrile at 298.15 K, 303.15 K and 308.15 K respectively.

T/K	$\Lambda_o \cdot \eta \cdot 10^4$/ S·m²·mol⁻¹mPa	$\Delta G^\circ \cdot 10^{-3}$/ kJ·mol⁻¹
298.15	66.07	-16.29
303.15	66.85	-16.26
308.15	67.11	-16.24

Table X.4: Limiting Ionic Conductance ($\lambda_0^{\pm}$), Ionic Walden Product ($\lambda_0^{\pm}\eta$) , Stokes' Radii (r_s), and Crystallographic Radii (r_c) of [bmpy]PF_6 in ACN at 298.15 K, 303.15 K and 308.15 K respectively.

T/K	ion	$\lambda_0^{\pm}$ (S·m²·mol⁻¹)	$\lambda_0^{\pm}\eta$ (S·m²·mol⁻¹mPa)	r_s (Å)	r_c(Å)
298.15	$Bmpy^+$	88.58	31.00	3.21	2.27
	PF_6^-	101.99	35.70	2.23	1.99
303.15	$Bmpy^+$	92.12	31.32	3.19	2.28
	PF_6^-	105.52	35.87	2.22	2.01
308.15	$Bmpy^+$	95.43	31.49	3.18	2.29
	PF_6^-	108.95	35.95	2.20	2.02

Table X.5: Average computed thermodynamic parameters for [bmpy]PF_6 in Acetonitrile.

ΔG_a^0 / kJ·mol⁻¹	ΔH_a^0 / kJ·mol⁻¹	ΔS_a^0 / J K⁻¹mol⁻¹	E_a/ kJ·mol⁻¹
-16.29	9.28	85.76	5.69

Table X.6: The calculated limiting molal conductance of ion-pair (Λ_0), limiting molar conductances of triple ion Λ_0^T, experimental slope and intercept obtained from Fuoss-Kraus Equation for [bmpy]PF_6 in THF and DO at 298.15 K, 303.15 K and 308.15 K respectively.

Solvents	$\Lambda_0 \cdot 10^4$ /S·m²·mol⁻¹	$\Lambda_o^T \times 10^4$ /S·m²·mol⁻¹	Slope×10⁻²	Intercept ×10⁻²
		298.15 K		
THF	44.86	29.92	0.18	-5.25
1,3 DO	36.31	24.22	0.11	-6.95
		303.15 K		
THF	48.64	32.44	0.37	-5.48
1,3 DO	38.49	25.67	0.28	-7.02
		308.15 K		
THF	54.51	36.36	0.57	-5.70
1,3 DO	43.53	29.03	0.44	-7.91

Table X.7: Salt concentration at the minimum conductivity (C_{min}) along with the ion-pair formation constant (K_P), triple ion formation constant (K_T) for [bmpy]PF_6 in THF and 1,3 DO at 298.15 K, 303.15 K and 308.15 K respectively.

Solvents	$c_{min} \cdot 10^4$/ mol·dm⁻³	log c_{min}	$K_P . 10^2$/ (mol·dm⁻³)⁻¹	$K_T . 10^3$/ (mol·dm⁻³)⁻¹	$K_T / K_P . 10^5$	log K_T / K_P
			298.15 K			
THF	5.45	0.7364	5.59	58.54	10.47	1.019
1,3 DO	5.26	0.7209	5.28	63.25	11.98	1.078
			303.15 K			
THF	7.49	0.8745	5.29	65.19	12.32	1.090
1,3 DO	5.46	0.7372	5.18	68.85	13.29	1.123

			308.15 K			
THF	7.54	0.8774	5.08	67.05	13.19	1.120
1,3 DO	5.49	0.7396	5.05	71.86	14.23	1.153

Table X.8: Salt concentration at the minimum conductivity (c_{min}), the ion pair fraction (α), triple ion fraction (α_T), ion pair concentration (c_P) and triple-ion concentration (c_T) for [bmpy]PF_6 in THF and DO at 298.15 K, 303.15 K and 308.15 K respectively.

Solvents	$c_{min}\cdot10^4$/ mol·dm^{-3}	$\alpha\cdot10^{-2}$	$\alpha_T\cdot10^2$	$c_P\cdot10^{-3}$/ mol·dm^{-3}	$c_T\cdot10^{-2}$/ mol·dm^{-3}
			298.15 K		
THF	6.93	15.14	59.42	0.98	3.24
DO	5.26	17.50	61.41	0.97	3.23
			303.15 K		
THF	6.91	15.32	74.79	1.69	5.60
DO	5.38	18.45	65.78	1.08	3.59
			308.15 K		
THF	6.89	18.62	76.58	1.73	5.77
DO	5.09	17.21	67.89	1.12	3.73

Table X.9: Limiting apparent molal volume (ϕ_V^0), experimental slope (S_v^*), viscosity -*B* and -*A* coefficient for [bmpy]PF_6 in ACN, THF and DO at 298.15 K, 303.15 K and 308.15 K respectively.

Solvents	$\phi_V^0\cdot10^6$/ m^3·mol^{-1}	$S_V^*\cdot10^6$/ m$^3\cdot$mol$^{-3/2}\cdot$dm$^{3/2}$	B/dm$^3\cdot$mol^{-1}	A/dm$^{3/2}\cdot$mol$^{-1/2}$
		298.15 K		
ACN	250.69	-123.17	1.6567	0.1069
THF	262.63	-130.94	1.6699	-0.0117

DO	271.10	-162.01	1.8868	-0.1540
		303.15 K		
ACN	258.73	-128.02	1.7741	0.1048
THF	275.96	-172.73	1.7790	-0.0188
DO	282.02	-163.90	2.0042	-0.1659
		308.15 K		
ACN	265.71	-129.58	1.9134	0.1036
THF	281.33	-177.27	1.9375	-0.0338
DO	288.72	-168.75	2.1761	-0.1757

Table X.10: Values of empirical coefficients (a_0, a_1, and a_2) of Equation 4 for IL in ACN, THF and DO.

solvents	$a_0 \cdot 10^6$ /m^3·mol^{-1}	$a_1 \cdot 10^6$ /m^3·mol^{-1}·K^{-1}	$a_2 \cdot 10^6$ /m^3·mol^{-1}·K^{-2}
ACN	-2144.9	14.356	-0.0212
THF	-14921.0	98.393	-0.1592
DO	-8008.5	52.934	-0.0844

Table X.11: Limiting apparent molal expansibilities (ϕ_E^0) for IL in different solvents (ACN, THF and DO) at 298.15K to 308.15K respectively.

solvent mixture	$\phi_E^0 \cdot 10^6$ /m^3·mol^{-1}·K^{-1}			$\left(\partial\phi_E^0/\partial T\right)_P \cdot 10^6$ /m^3·mol^{-1}·K^{-2}
ACN+IL				
T/K	298.15	303.15	308.15	
	1.714	1.502	1.290	-0.042

THF+IL				
T/K	298.15	303.15	308.15	
	3.462	1.870	0.278	-0.318

DO+IL				
T/K	298.15	303.15	308.15	
	2.606	1.762	0.918	-0.168

Table X.12: Stretching frequencies of the functional groups present in the pure solvent and change of frequency after addition of IL in the solvents.

	Stretching frequencies		
Solvents	Functional Group	Pure Solvent (ν_o cm^{-1})	{(bmpy)PF_6+Solvents} (ν_{IL} cm^{-1})
CH_3CN	C≡N	2253.2	2275.1
	C-H	2918.9	2922.3
THF	C-O	1043.1	1062.4
	C-H	2914.3	2917.2
DO	C-O	1158.2	1175.5
	C-H	2915.7	2918.2

FIGURES

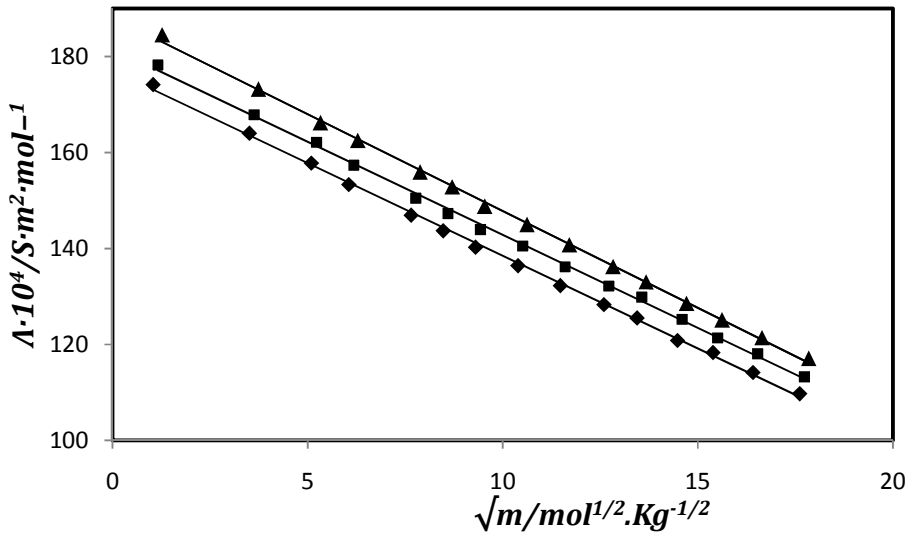

Figure X.1: Plot of molal conductance (Λ) versus $\sqrt{m}$ for [bmpy]PF_6 in ACN at 298.15 K (♦), 303.15 K (■) and 308.15 K (▲).

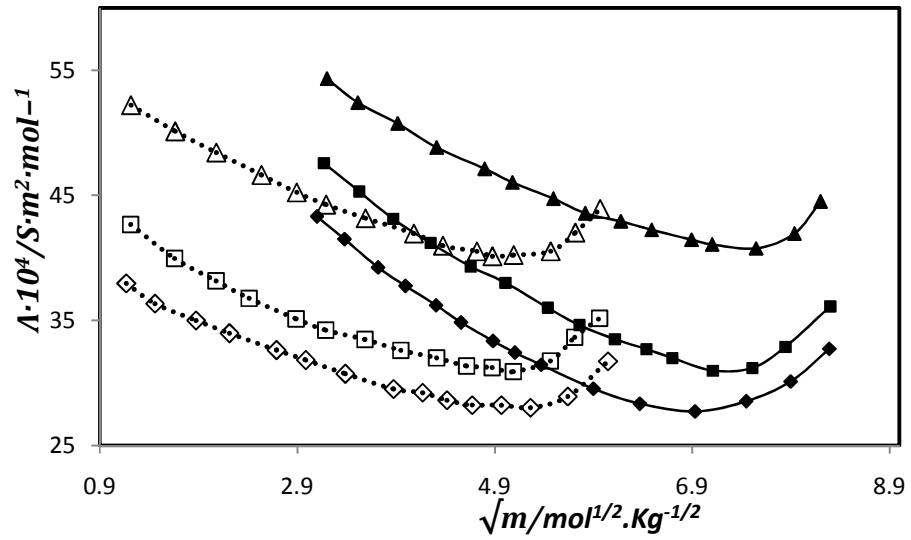

Figure X.2: Plot of molal conductance (Λ) versus $\sqrt{m}$ for [bmpy]PF_6 in THF at 298.15 K (♦), 303.15 K (■), 308.15 K (▲) and in DO at 298.15 K (◊), 303.15 K (□),308.15 K (Δ).

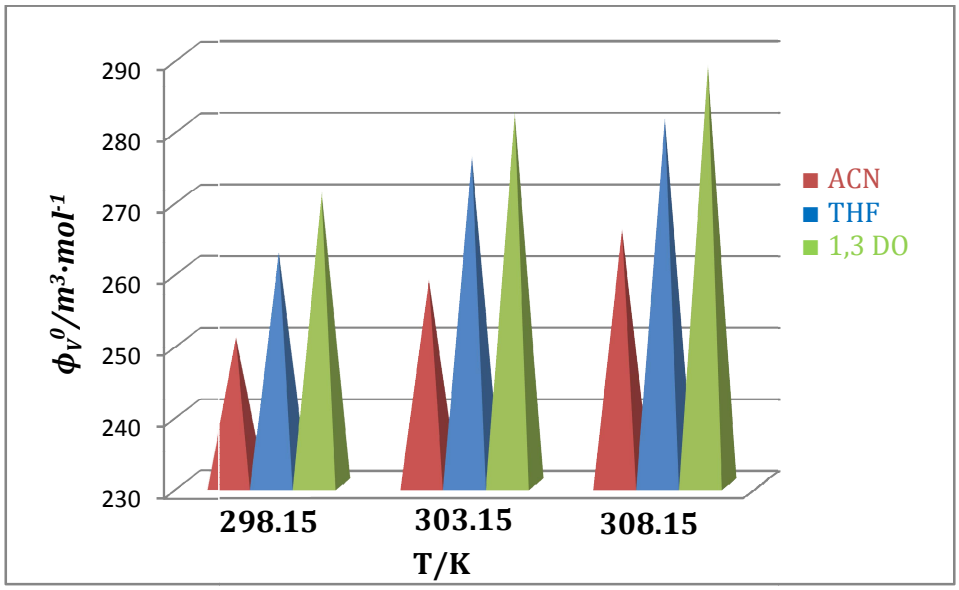

Figure X.3: Plot of temperature versus limiting apparent molal volume (Φ_v^0) for [bmpy]PF_6 in ACN (red) , THF (blue) and 1,3 dioxolane (green).

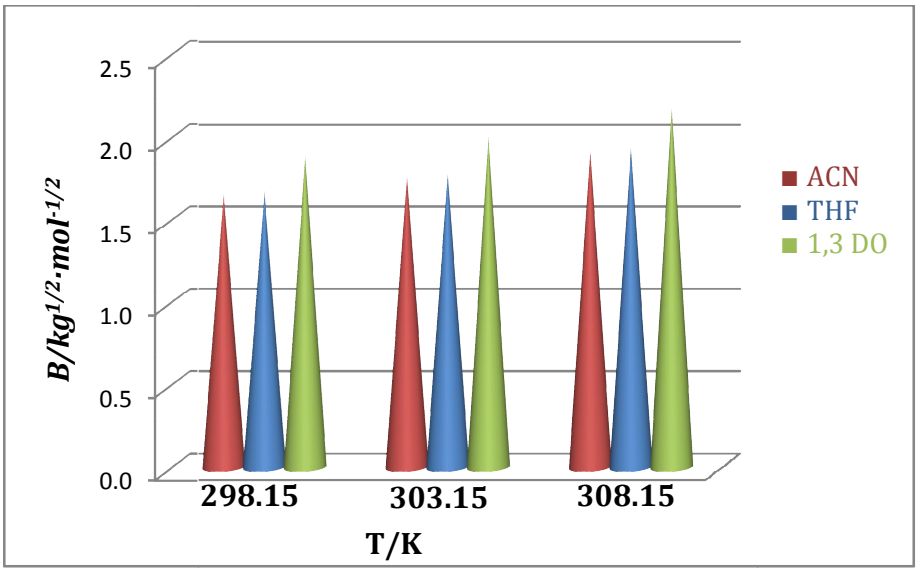

Figure X.4: Plot of temperature versus Viscosity *B*-Coefficient for [bmpy] PF_6 in ACN (red), THF (blue) and 1,3 dioxolane (green).

SCHEMES

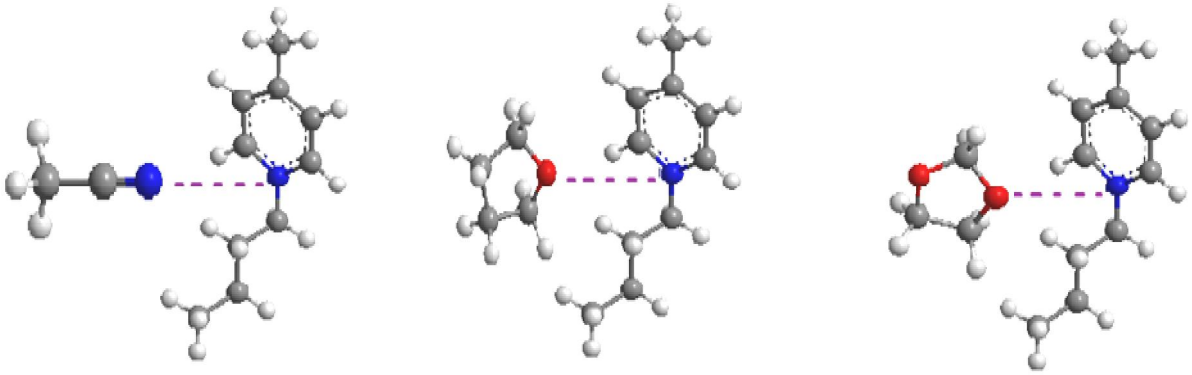

ACN IL THF IL 1,3 DO IL

Scheme X.1. **Plausible interfaces between the ionic liquid and diverse solvent systems.**

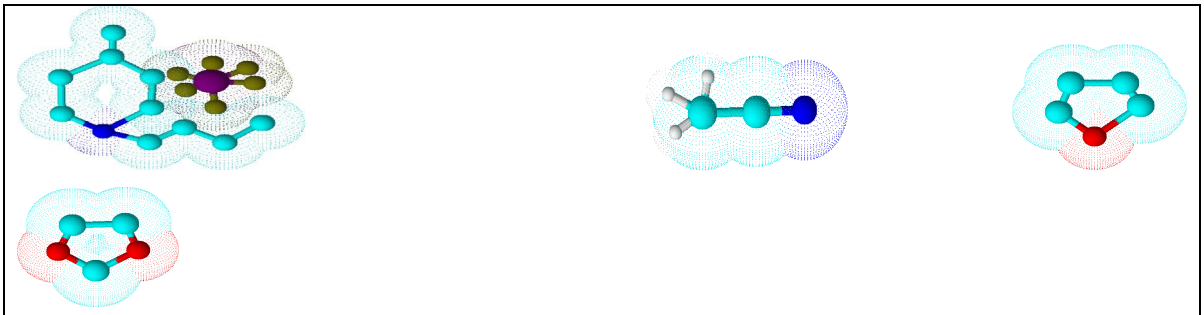

IL-1-butyl-4-methylpyridinium hexafluorophosphate ACN THF DO

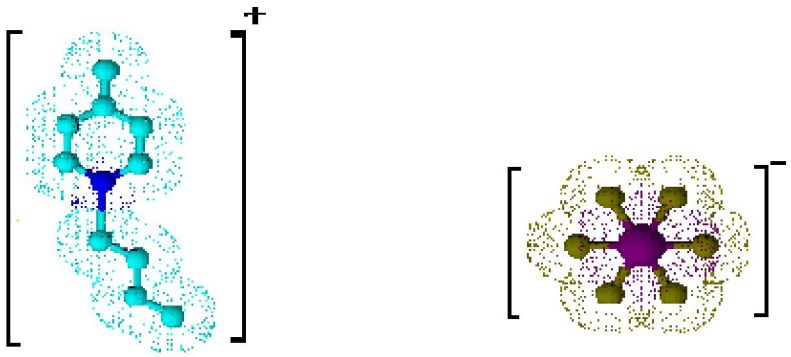

1-butyl-4-methyl pyridinium ion **Hexafluorohophate ion**

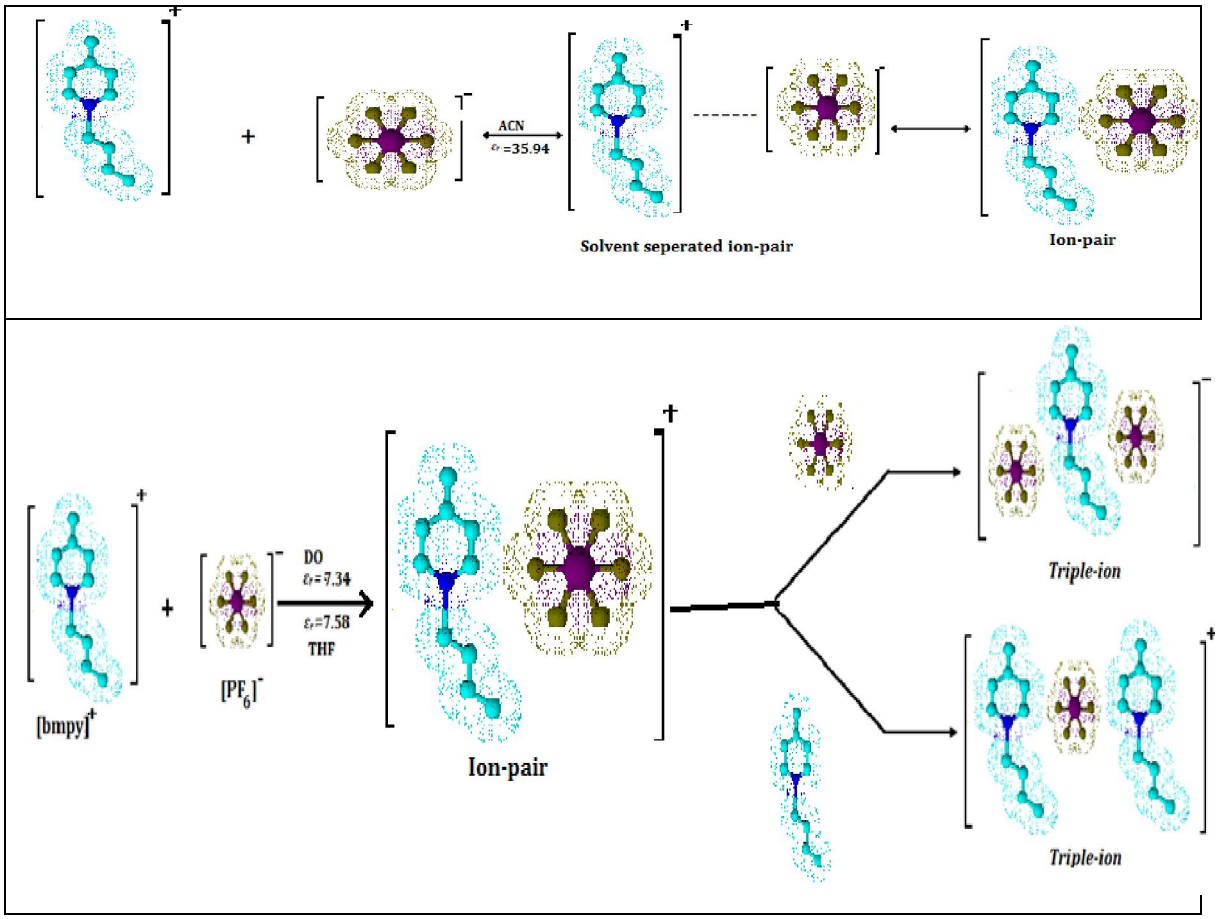

Scheme X.2. Molecular structures of the IL and the solvents and pictorial representation of ion-pair and triple-ion formation for the electrolyte in diverse solvent systems.

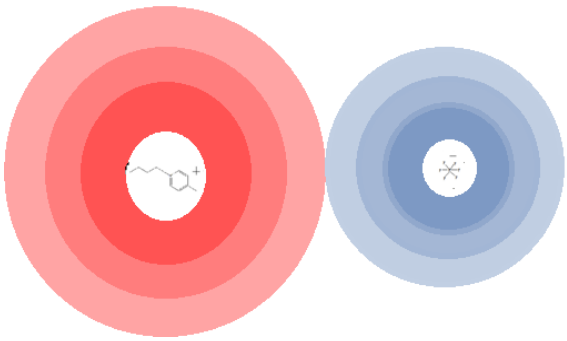

Scheme X.3. Electrostatic Forces of Attraction.

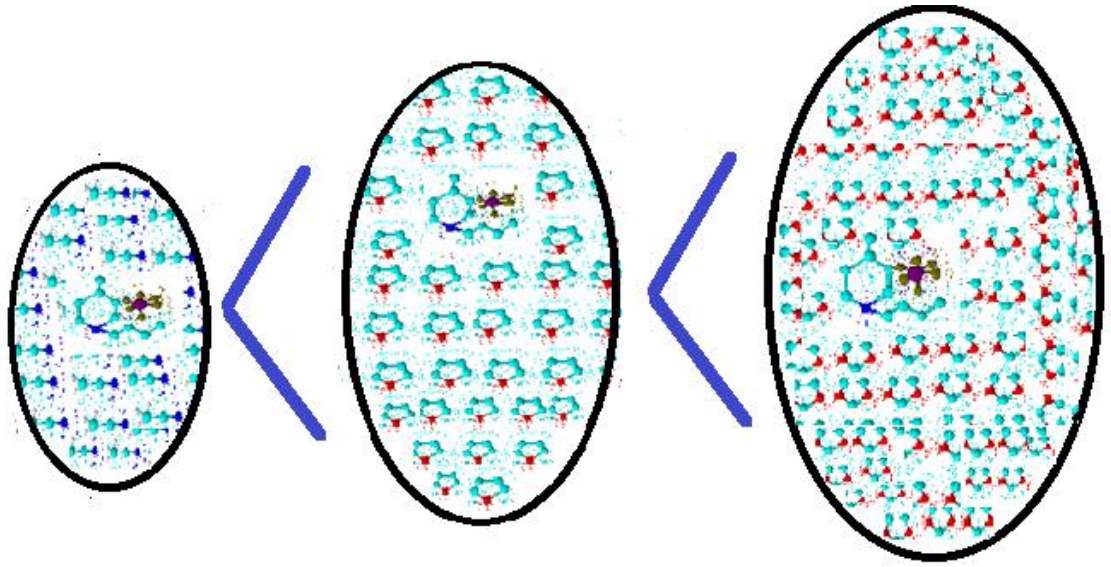

Scheme X.4. Extent of ion-solvent interaction of IL in miscellaneous solvent systems